

S1

Supplementary Information

Glycosyldiselenides as lectin ligands detectable by NMR in biofluids

Ignacio Pérez-Victoria,[‡] Omar Boutureira,[‡] Timothy D. W. Claridge*
and Benjamin G. Davis*

*Department of Chemistry, Chemistry Research Laboratory, University of
Oxford, Mansfield Road, Oxford OX1 3TA, UK.*

E-mail: ben.davis@chem.ox.ac.uk, tim.claridge@chem.ox.ac.uk

Table of Contents

- S2.** General considerations
- S2.** NMR assignments of bis(β -D-GlcpNAc)diselenide (**1**)
- S3.** Sample preparation for ligand-binding NMR experiments
- S3.** STD-NMR measurements
- S4.** 1D Tr-NOESY measurements
- S5.** Determination of K_D for the WGA:**1** complex by NMR titration
- S6.** Molecular modelling of bis(β -D-GlcpNAc)diselenide (**1**)
- S7.** Molecular docking simulations with AutoDock Vina
- S11.** Complete Relaxation and Conformational Exchange Matrix (CORCEMA-ST) calculations
- S12.** ^1H and ^{77}Se NMR measurements with a solution of **1** in rabbit plasma
- S13.** References

[‡]Present address: *Fundación MEDINA, Centro de Excelencia en Investigación de Medicamentos Innovadores en Andalucía, Avda. del Conocimiento 3, Parque Tecnológico de Ciencias de la Salud, E-18160 Armilla, Granada, Spain (I.P.-V) and Department of Chemistry, University of Cambridge, Lensfield Road, Cambridge CB2 1EW, UK (O.B).*

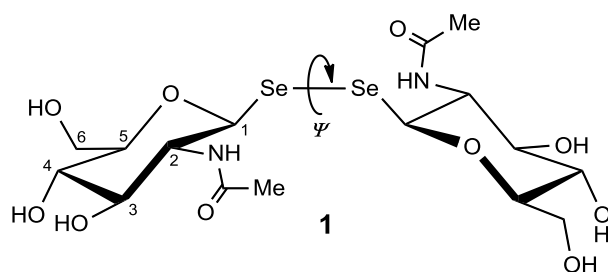
General considerations

Bis(β -D-GlcpNAc)diselenide (**1**) was synthesized as already reported.¹ Lectin from *Triticum vulgaris* [Wheat-germ agglutinin (WGA)], lyophilized rabbit plasma (containing 3.8% trisodium citrate as anticoagulant) and TSP [3-(Trimethylsilyl)propionic-2,2,3,3- d_4 acid sodium salt] were from SIGMA. The deuterated buffer was prepared by dissolving K_3PO_4 in D_2O (25 mM final concentration) and adjusting pH* to 5.3 with DCl (SIGMA), to this solution, TSP was added at a final concentration of 0.1 mM. This was the buffer employed to prepare all NMR samples but the plasma sample which was prepared in D_2O .

NMR experiments were carried out in different spectrometers and all spectra were processed with TOPSPINTM software. STD NMR experiments were recorded at 298 K on a Bruker AVII 500 spectrometer equipped with a 5mm z-gradient triple resonance inverse $^1H/^{13}C(^{19}F)$ TXI probe. 1H NMR spectrum for resonance assignment of glycosyldiselenide **1**, 1D NOESY and 1D Tr-NOESY experiments and the NMR titration experiments were recorded at 298 K on a Bruker AVIII 700 spectrometer equipped with a 5mm inverse TCI cryoprobe. 1H and ^{77}Se NMR experiments with the solution of **1** in reconstituted rabbit plasma were recorded at 298 K on a Bruker DRX500 spectrometer equipped with a 5-mm broadband BBO probe.

Molecular modelling of glycosyldiselenide **1** and the protein and ligand preparations for molecular docking were carried out with Accelrys Discovery Studio and AutoDock Tools (ADT) software. Molecular docking of **1** into the selected primary binding site of WGA was carried out with AutoDock Vina software.² All structural figures were prepared with PyMol.³

NMR assignments of bis(β -D-GlcpNAc)diselenide (**1**)



Proton NMR assignment for **1** was carried out by means of 1H , COSY and HSQC spectra acquired for a solution of **1** (5 mM) dissolved in the deuterated phosphate buffer. Prochirality of diastereotopic protons at C-6 was determined based on their chemical shifts and coupling constants according to the data in the literature.⁴ For example, typically for the D-*gluco*-series

saccharides, the signals of the H-6_{proR} proton are more shielded than those of H-6_{proS} ($\delta_{H6S} > \delta_{H6R}$), and J_{H5-H6R} coupling constants have higher values than J_{H5-H6S} .

¹H NMR (D₂O buffer, 700 MHz): δ = 5.043 (d, 1H, J_{1-2} = 10.5 Hz, H-1), 3.945 (dd, 1H, J_{1-2} = J_{2-3} = 10.2 Hz, H-2), 3.921 (dd, 1H, J_{6S-6R} = 12.6 Hz, J_{6S-5} = 1.8 Hz, H-6_S), 3.800 (dd, 1H, J_{6R-6S} = 12.6 Hz, J_{6R-5} = 4.7 Hz, H-6_R), 3.600 (dd, 1H, J_{2-3} = J_{3-4} = 9.2 Hz, H-3), 3.517 (dd, 1H, J_{3-4} = 9.4 Hz, J_{4-5} = 9.4 Hz, H-4), 3.491 (m, 1H, H-5), 2.050 (s, 3H, MeCONH-) ppm.

Sample preparation for ligand-binding NMR experiments

Commercial WGA lectin as lyophilised powder was reconstituted at *ca.* 8 mg/ml in the deuterated phosphate buffer (at pH* 5.3 the protein is in its native dimeric state)⁵. After spinning to pellet any insoluble material, the protein concentration in the supernatant was measured with a NanoDrop[®] spectrophotometer reading at 280 nm [protein parameters set to MW = 36 kDa (dimer) and $\epsilon_{280} = 1.09 \times 10^5 \text{ M}^{-1} \text{ cm}^{-1}$]⁶ to give a value of 210 μM (7.56 mg/ml). It is important to note that commercial WGA is comprised of three isoforms (35% WGA I, 55% WGA II and 10% WGA III) with small variations in peptide sequence (5–8 residues in 171 amino acids).⁷ Glycosyldiselenide **1** was dissolved in the deuterated buffer at a final concentration of 30 mM. Using these stocks solution, the sample for STD and Tr-NOESY ligand-binding experiments was prepared with a final protein concentration [WGA] = 100 μM (0.4 mM primary binding sites concentration) and a carbohydrate concentration [**1**] = 5 mM. Thus, the protein – ligand molar ratio was 1:50, corresponding to 1:12.5 with respect to the primary binding sites concentration.

STD-NMR measurements

STD experiments were performed at 298 K using the standard STD pulse sequence of the spectrometer library *stdiff* using a train of Gaussian shaped pulses (50 ms, 90°) for selective protein irradiation, and an alternation between on and off resonances.⁸ The on-resonance frequency was set to 6.8 ppm as described in previous STD NMR experiments involving WGA,⁹ and the off-resonance frequency was set to 40 ppm where no NMR resonances of ligand or protein are present. Relaxation delay was 4 s and acquisition time 3 s. Appropriate blank experiments were carried out to ensure the lack of direct saturation of the ligand protons. A saturation time of 2.5 s was chosen. The total number of scans was 3200.

1D Tr-NOESY measurements

Interannular NOEs of disaccharides and disaccharide mimetics are relevant with regard to the conformations about the interglycosidic bond. Nevertheless, due to the symmetry of glycosyldiselenide **1**, no interannular NOEs are available for this sugar as already described for symmetrical glycosyldisulfides.¹⁰ In any case, as a further evidence for binding, 1D NOESY experiments were carried out with glycosyldiselenide **1** in the presence and the absence of lectin. Experiments were performed using the double-pulsed field gradient sculpted excitation (DPFGSE) NOESY sequence¹¹ with selective excitation of the magnetically equivalent anomeric protons (H-1 and H-1'). Mixing time was set to 300 ms in the sample containing the lectin and 600 ms in the sample with just the free ligand. The Tr-NOESY effect, which unequivocally demonstrates binding, is clearly observed (Fig. S1) since in the presence of the lectin the peaks of the selectively excited resonance and its NOE partners share the same sign while in the absence of the protein they have opposite sign.¹²

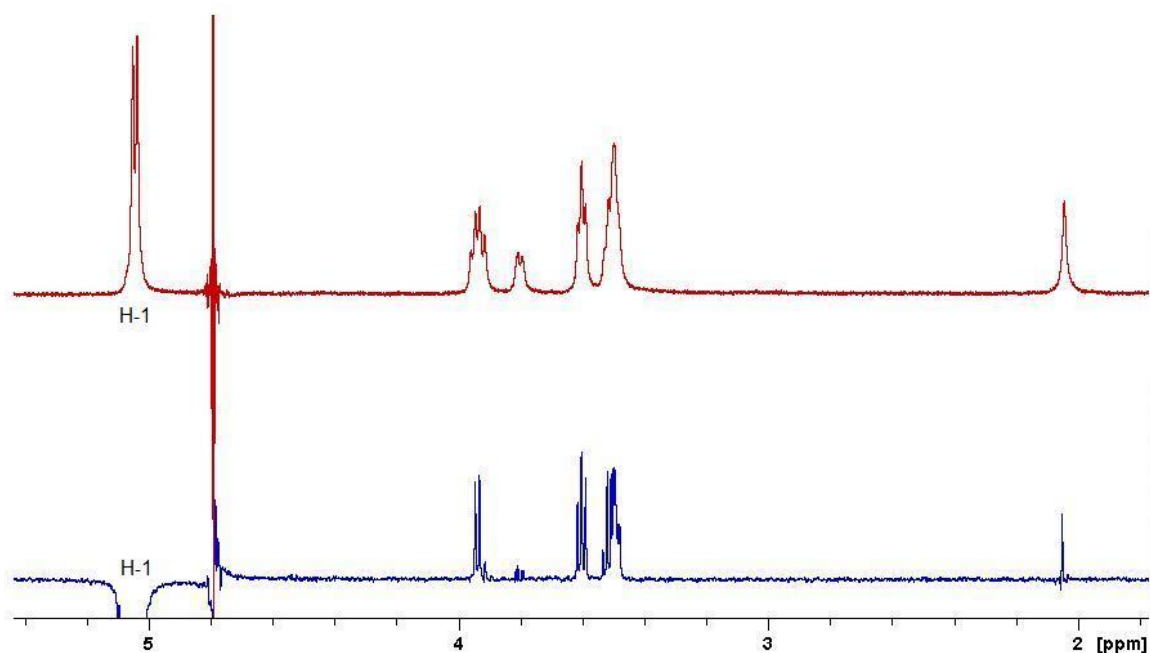


Fig. S1 1D Tr-NOESY spectrum of glycosyldiselenide **1** with selective excitation of the resonance from H-1 in the presence of WGA (red spectrum) and the reference 1D NOESY spectrum of **1** in absence of the lectin (blue spectrum). Mixing time was set to 300 ms for the sample with the lectin and 600 ms for the free ligand sample. The spectra were recorded at 700 MHz.

Determination of K_D for the WGA:1 complex by traditional NMR titration

In order to determine the strength of binding of **1** to WGA and compare it to the reported values for GlcNAc, a titration of the ligand into the protein was followed by ^1H NMR. Using the previously indicated stocks solution for WGA and **1**, the ligand was titrated over the lectin. WGA concentration was kept constant at 100 μM , while the carbohydrate concentration varied from 1.5 mM to 15.7 mM in the following way:

[1] / mM	1.5	3.0	5.0	7.0	10.0	12.0	15.7	3.0
[WGA] / μM	100	100	100	100	100	100	100	0
Linewidth / Hz	23.6	17.0	11.55	9.6	7.6	6.3	5.4	1.3

A sample with just ligand (5 mM) but no protein was also prepared in the same buffer. Each titration point was prepared separately in a total volume of 200 μL . The titration samples were transferred to 3 mm NMR capillary tubes (filled with 175 μL). After acquiring the corresponding ^1H NMR spectra, the K_D was determined by analysing the line width of the *N*-acetyl methyl resonance versus ligand concentration as already reported.⁵ Line width at half-height of the selected singlet was obtained after fitting the peak to a perfect Lorentzian shape using TOPSPINTM software (Bruker) tools for peak deconvolution.

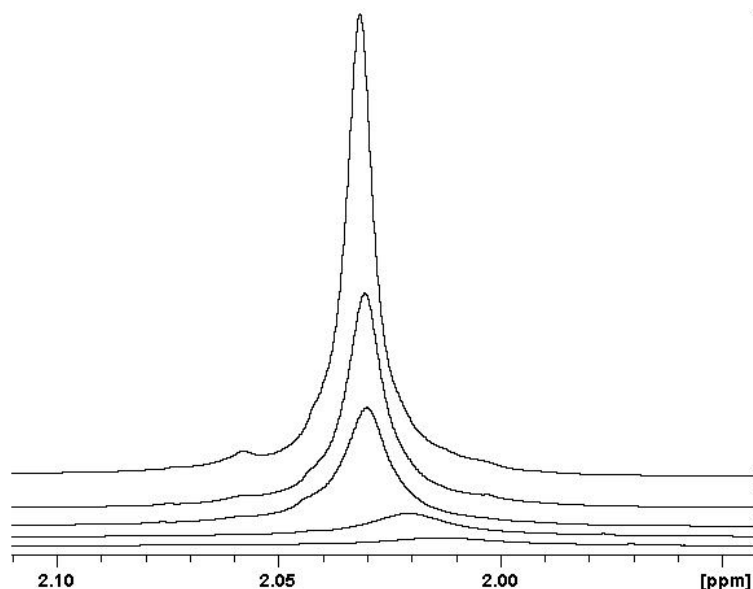


Fig. S2. 700 MHz ^1H NMR spectra of selected titration points showing the *N*-acetyl methyl resonance in the ligand at different concentrations (15.7 mM, 10 mM, 7 mM, 3 mM and 1.5 mM from top to bottom respectively) while keeping constant the lectin concentration (100 μM).

When a ligand rapidly exchanges between a protein binding site and solvent, the observed line width (ν_{obs}) of various ligand resonances can differ from the width seen in the absence of

protein (ν_{free}). A similar behaviour happens with chemical shifts ($\Delta\delta$). Under conditions where the fraction of ligand bound to protein is small, the dissociation constant K_D is given by the following equation:¹³

$$[L]_{\text{TOT}} = \Delta\nu_B \cdot ([P]_{\text{TOT}} / \Delta\nu) - K_D$$

Where $\Delta\nu = \nu_{\text{obs}} - \nu_{\text{free}}$, $[P]_{\text{TOT}}$ is the total concentration of protein binding sites, $[L]_{\text{TOT}}$ is the total ligand concentration and $\Delta\nu_B$ is the apparent line width change relative to that of the free ligand for the ligand in the bound state. The corresponding equilibrium dissociation constant is easily derived from the ordinate intercept in the $[L]_{\text{TOT}}$ vs. $1/\Delta\nu$ plot.

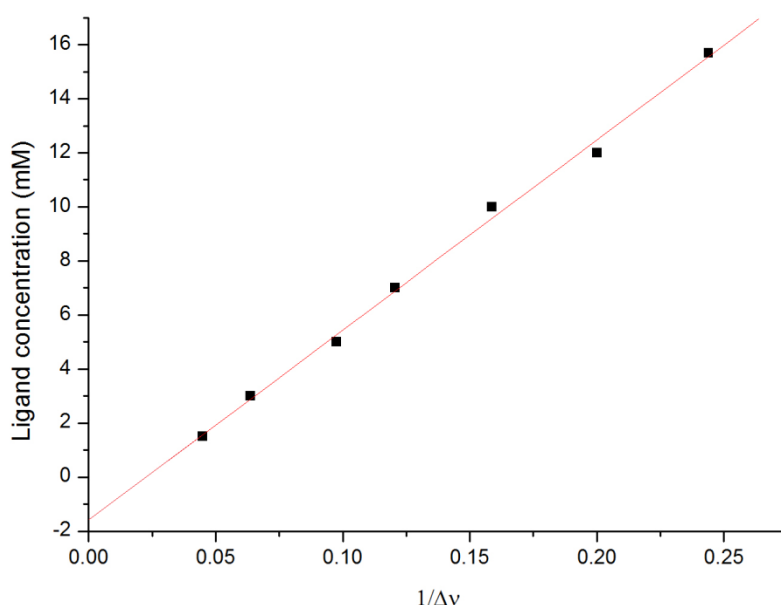


Fig. S3 Binding of glycosyldiselenide **1** to WGA. Plot of $[L]_{\text{TOT}}$ vs. $1/\Delta\nu$ of the *N*-acetyl resonance of the ligand **1** according to the previous equation.

Analysis of the fitted line (Fig. S3) gives a value of K_D equal to 1.6 mM which compares well with the 2.2 mM reported for GlcNAc determined in the same way (and at the same pH*).⁵ The line fitting was very good with a correlation factor $r^2 = 0.996$.

Molecular model of bis(β -D-GlcpNAc)diselenide (**1**)

From the most recently reported X-ray structure of WGA: β -GlcNAc complex,¹⁴ the monosaccharide was copied to construct glycosyldiselenide **1**. The anomeric hydroxyl group in this extracted β -GlcNAc was substituted by a Se atom, and this selenylglycoside unit was dimerized via the formation of a Se-Se bond. The reported crystal structure for the peracetylated bis(β -D-glucopyranosyl) diselenide,¹⁵ was employed for setting the same interglycosidic bond angles and lengths in the following way:

$d(\text{Se-Se}) = 2.325 \text{ \AA}$; $d(\text{Se-C1}) = 1.960 \text{ \AA}$; $\theta(\text{Se-Se-C1}) = 101^\circ$; $\psi(\text{C1-Se-Se-C1}') = -82^\circ$; the $\text{C2-C1-Se-Se-C1}'\text{-C2}'$ backbone was set with an *anti-syn* geometry with torsional angles $\phi(\text{C2-C1-Se-Se}) = 179^\circ$ and $\phi(\text{Se-Se-C1}'\text{-C2}') = -69^\circ$.

The resulting structure was not force field minimized but used directly as input structure for the molecular docking calculations.

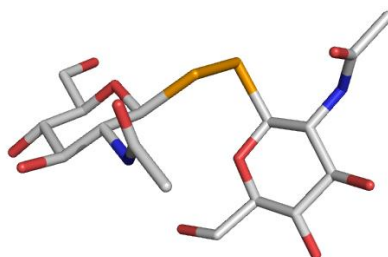


Fig. S4 Molecular model of glycosyldiselenide **1** (hydrogen atoms are omitted for clarity).

Molecular docking simulations with AutoDock Vina

Docking calculations were performed with AutoDock Vina.² This program combines some advantages of knowledge-based potentials and empirical scoring functions. It extracts empirical information from both the conformational preferences of the receptor-ligand complex and from experimental affinity measurements. Autodock Vina uses a sophisticated gradient optimization method for its local optimization procedure. This docking program also improves the accuracy of the binding mode predictions obtained with the popular AutoDock 4 program,¹⁶ and it is two-order of magnitude faster.² The interaction of WGA with *N*-acetylglucosamine and a number of its derivatives has already been successfully studied by molecular docking using AutoDock 3.0.¹⁷ Such study also found an excellent linear correlation of the predicted binding free energies with the experimental data. For this reason and based in its improved performance compared to AutoDock 4.0, AutoDock Vina was the software chosen for the molecular docking simulations involving WGA and glycosyldiselenide **1**. Since selenium is not parameterised within the Autodock force field, its atom parameters were exchanged for those of sulphur in the docking calculations, as recommended by the Autodock developers. Such a change seems reasonable due to their similarity of van der Waals radii (1.9 \AA for Se and 1.8 for S) and electronegativities (2.48 for Se and 2.44 for S, Pauling scale).

As already indicated, commercial WGA is comprised of three isoforms (35% WGA I, 55% WGA II and 10% WGA III) with small variations in peptide sequence (5–8 residues in 171 amino acids).⁷ The protein for the docking calculations was prepared starting from the most recently reported crystal structure of the complex between WGA and β -GlcNAc.¹⁴ The

actual isolectin in this complex is WGA I (PDB ID: 2UVO). The unit cell in this X-ray structure contains a pair of protein dimers; one of them was removed to continue working with just a protein dimer. The bound carbohydrate molecule in one of the four primary binding sites (there are two per protein monomer and these sites are located at the monomer-monomer interface) was selected as the place where further docking was going to be carried out. Then all the crystallographic water molecules were removed except those identified as important for β -GlcNAc binding (bridging protein and ligand via hydrogen bonding) in the chosen primary binding site. Afterwards all the bound carbohydrate molecules and the glycerol molecule present in the crystallographic structure were also removed. This left a structure of isolectin WGA I as apo- form containing just the key water molecules required for β -GlcNAc binding in the selected primary binding site. Later, five amino acids were modified (T56P, Q59H, Y66H, A93S, and G171A) to obtain a model of WGA II. This was carried out since this isolectin is the main one in the commercial WGA employed for the experimental work. This same approach has been already described in the NMR and molecular modelling studies of the interaction between WGA and β -D-GlcpNAc-(1 \rightarrow 6)- α -D-ManpOMe using the same commercial preparation of the lectin.⁹ After these *in silico* mutations, the residues were locally minimized. Only the new H66 is located in the primary binding site and, after the local minimization, it was checked that the aromatic rings in the new histidine and the former tyrosine residues were coplanar and located in the same place. This apo- form of the isolectin WGA II (from now on named “apoWGA”) was then further prepared for docking using AutoDock Tools 1.5.4. With this program, polar hydrogens were added to the protein receptor and the search space (“Grid box”) for docking was defined. The search space was centred where the β -GlcNAc is located in the previously chosen primary binding site and the dimensions of the Grid box were defined to 24 \times 24 \times 24 Å. The prepared apoWGA was treated as a rigid receptor for the docking simulations.

For the preparation of the ligand to be docked, the previously created molecular model of glycosyldiselenide **1** was opened in Autodock Tools 1.5.4 for merging its non-polar hydrogens leaving just the polar ones. The pyranose ring bonds were kept rigid while all the open-chain bonds were treated as active torsional bonds. For this reason, it was not required any accuracy in the value of the torsional interglycosidic angle Ψ (C–Se–Se–C) in the input structure of glycosyldiselenide **1** since all the conformational space for this torsion is actually explored in the docking simulations. Once the ligand (**1**) and receptor (apoWGA) were properly prepared and the search space was defined, the molecular docking simulations were carried out with AutoDock Vina.² Docking was carried out with an exhaustiveness value of 16

and a maximum output of 25 structures. We first validated docking with AutoDock Vina by testing its ability to predict the β -GlcNAc binding mode seen in the crystal structure of the complex with WGA I (PDB ID: 2UVO)¹⁴. The β -GlcNAc molecule extracted from the complex structure was directly docked in the previously defined Grid box of apoWGA. The generated lowest energy pose predicted by AutoDock Vina reproduced very accurately the binding mode seen in the crystal with an RMSD = 0.7916 Å. In spite of the Y66H virtual mutation to turn crystallographic WGA I into the model of WGA II (apoWGA), the docking simulation worked nicely. This is not surprising since both aromatic rings (Y66 in crystallographic WGA I and H66 in modelled WGA II) were coplanar and located at the same place as previously indicated.

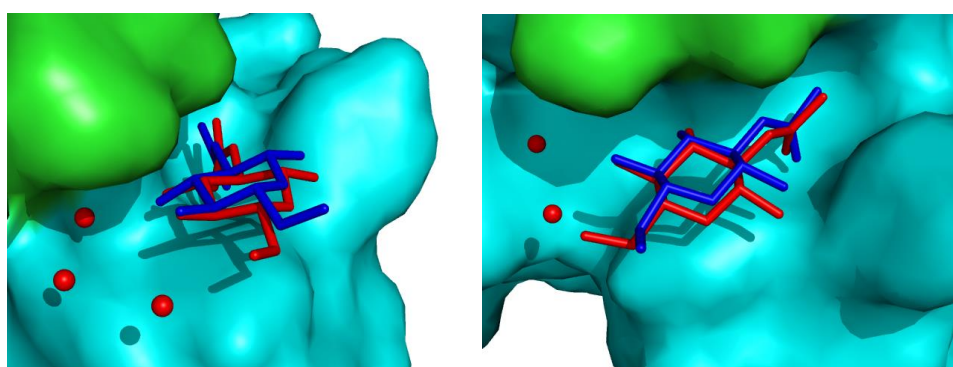


Fig. S5 Two views showing the overlay of crystallographic β -GlcNAc (red) and its lowest energy docking binding model (blue) in the selected primary binding site of WGA. Hydrogens are omitted for clarity. Water molecules included in the simulations are represented as red spheres. Protein monomeric chains are shown as surface representation in green and cyan colours.

After the validation of the molecular docking procedure with the control ligand (crystallographic β -GlcNAc), the simulations were carried out using the modelled glycosyl diselenide **1** as input ligand structure and the same prepared protein receptor (apoWGA) using the same level of exhaustiveness in AutoDock Vina. The three lowest energy docking poses displayed predicted binding affinities of -6.7 kcal/mol (pose 1) and -6.3 kcal/mol (poses 2 and 3). All three located one of the residues in the same site where the corresponding monosaccharide is found in the crystal structure of its complex with WGA,¹⁴ as already observed in the validating docking simulation with the control ligand previously described. The other GlcNAc residue in **1** is located closer to TYR64 (chain B) and GLU115 (chain A) in pose 1 (Ψ equal to -82.6°) and closer to GLN49 (chain B) and ARG45 (chain B) in poses 2 (Ψ equal to $+109.3^\circ$) and 3 (Ψ equal to $+90.2^\circ$). These later two poses are indeed very similar with just a 180° torsional rotation difference around the C–Se bond of the second residue. The remaining generated poses displayed predicted binding affinities ≥ -6.0 kcal/mol and many of

them had unreasonable values of interglycosidic dihedral angle Ψ (far away from $+90^\circ$ or -90° which is the average value reported for analogous glycosyldisulfides)¹⁰ or even did not locate the first residue in the location of crystallographic β -GlcNAc. Thus, only the mentioned three lowest energy docking poses were considered as plausible binding modes for ligand **1** in WGA primary binding site. On the other hand, as already mentioned, Neumann and co-workers found an excellent linear correlation of the predicted binding free energies with the experimental data in the molecular docking study (using AutoDock 3.0) of the interaction of WGA with *N*-acetylglucosamine and a number of its derivatives.¹⁷ Thus it is reasonable to assume that such correlation will also be valid when using AutoDock Vina instead of AutoDock 3.0, since Vina performs more accurately. For this reason also, the three lowest energy docking poses we obtained have the highest probability to actually reflect the binding modes for ligand **1** in the primary binding site of WGA.

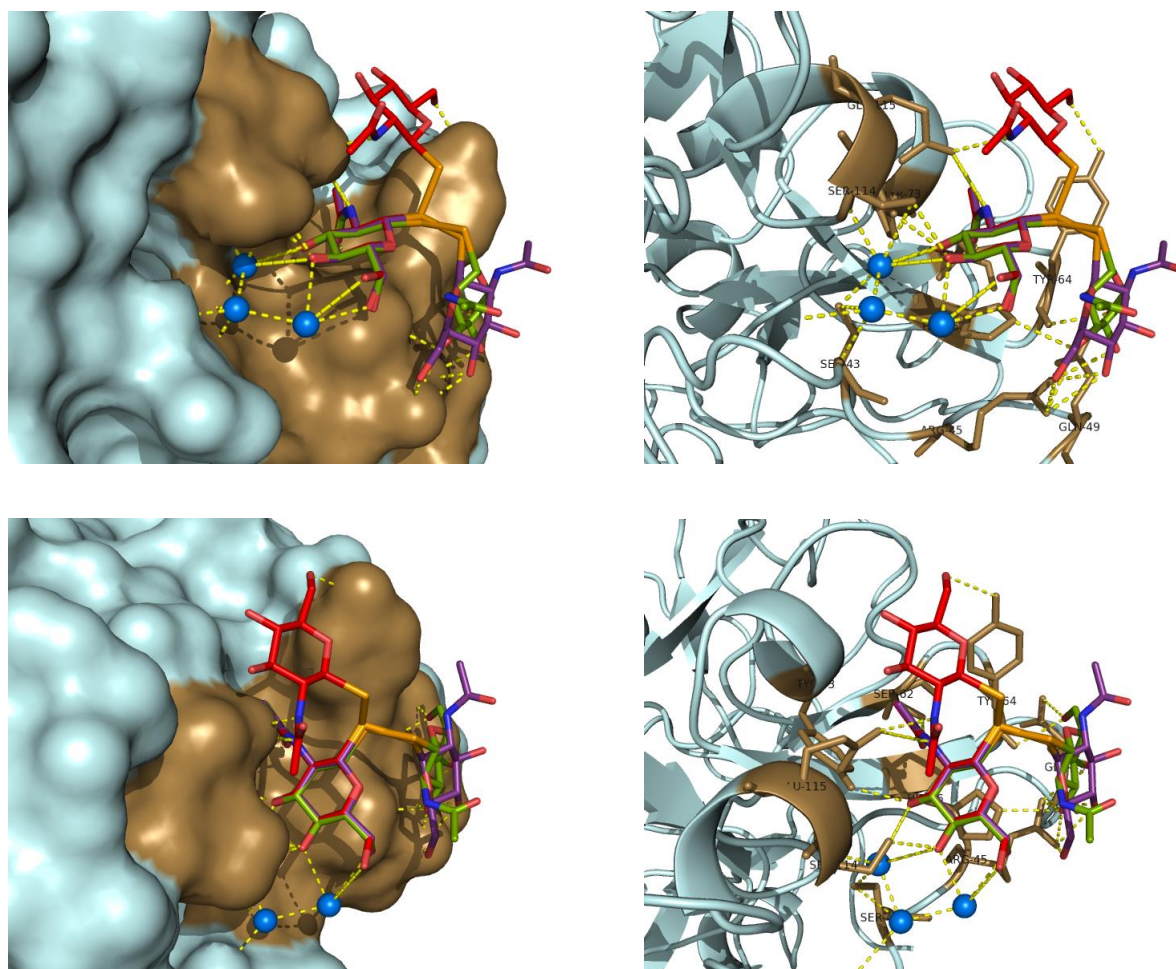


Fig. S6 Three main binding modes of glycosyl diselenide **1** in the primary binding site of WGA derived from docking calculations: pose 1 (red), pose 2 (green) and pose 3 (purple). Interacting amino acids are represented in sand color and polar contacts as yellow dashed lines. Water molecules included in the calculations are represented as blue spheres. Protein dimer is shown as surface (left) and ribbon/sticks (right) representation.

Complete Relaxation and Conformational Exchange Matrix (CORCEMA-ST) calculations

In order to determine which of the three lowest energy poses of glycosyl diselenide **1** corresponds to the actual binding mode, the experimental STD effects were compared with those calculated for each docking model by the program CORCEMA-ST.¹⁸

The Cartesian coordinates of the apoWGA used as protein receptor for the docking simulations were employed for the full relaxation matrix analysis. To reduce the dimensions of the matrixes, only amino acids within 8 Å around the ligand were considered in the CORCEMA-ST calculations. The ligand centre was defined at the anomeric carbon of the closest monosaccharide unit to the protein since this sugar residue was placed identically in the three lowest energy docking poses of **1**. As no chemical shift assignment of the protein protons was available, the selection of the irradiated protons was done using a SHIFTX 1.1 prediction of the chemical shift.¹⁹ All the protons within the [6.1–7.5] ppm range were included as irradiated to account for the effects of line broadening under the experimental conditions and also the excitation width of the selective pulse used. All exchangeable hydrogen atoms were excluded in the calculations, as the STD NMR experiments were performed in a D₂O buffer. We assumed that the coordinates for the bound and free protein were identical, and several iterative cycles were performed to reach the optimized parameters. The K_D previously determined via the NMR titrations (1.6 mM) was used for the calculations. For this protein–ligand system, the classical assumption of a diffusion limited association step (on-rate $10^8 \text{ M}^{-1} \text{ s}^{-1}$) was considered. This assumption is reasonable since the primary carbohydrate binding site of WGA is a shallow one. The order parameter for methyl –X relaxation S^2 was set to 0.85 and the relaxation leakage to 0.1 s^{-1} . The correlation time of the bound ligand ($\tau_{\text{r-protein}}$) was initially set to 30 ns, whereas 0.13 ns was used for the free ligand ($\tau_{\text{r-ligand}}$). These correlation time values were reported in a study of the molecular dynamics of GlcNAc bound to WGA by deuterium NMR.²⁰ The methyl group internal correlation time (τ_{m}) was set at a reasonable value of 5 ps.²¹ Nevertheless, the correlation times for free and bound ligand were optimized (to minimize the R -factor) for the lowest energy docking pose of **1** by iterative calculations and finally, the best parameters were found to be 65 ns for $\tau_{\text{r-protein}}$ and 2 ns for $\tau_{\text{r-ligand}}$. This might be considered an oversized value for the correlation time of a 36 kDa protein (WGA dimer). However, this seems to be not uncommon in CORCEMA-ST calculations,²² particularly when the protein shape deviates from a perfect globular shape, as is the case with the WGA dimer. Likewise, slightly higher than *a priori* expected values for $\tau_{\text{r-}}$

ligand are common in CORCEMA-ST calculations.²³ The input parameters were exactly the same for calculations involving the other two docking poses. The STD intensities for each docking pose were calculated as percentage fractional intensity changes, $S_{\text{calc},k}$, from the intensity matrix $I(t)$ ($S_{\text{calc},k} = (([I_{0k} - I(t)_k] * 100) / I_{0k})$, where k is a particular proton in the complex, and I_{0k} its thermal equilibrium value),^{18a} and the calculation was carried out for a saturation time of 2.5 s.

In order to determine which of the three lowest energy docking poses corresponded to the actual binding mode, the experimental STD effects were compared with those calculated for each docking model. The theoretical STD values were compared to the experimental ones using the NOE R -factor defined as:

$$R\text{-factor} = \sqrt{\frac{\sum (S_{\text{expt},k} - S_{\text{calc},k})^2}{\sum (S_{\text{expt},k})^2}}$$

where S_{expt} and S_{calc} refer to experimental and calculated STD effects for proton k , respectively. Due to the symmetry of ligand **1**, the calculated STD effects for the same relative proton in each GlcNAc residue of diselenide **1** were mean-averaged as already described for the CORCEMA-ST calculations with the symmetrical non-reducing disaccharide trehalose, a ligand of *E. coli* repressor protein TreR.²⁴ In the free state, which is the one STD NMR can observe, both GlcNAc residues are obviously chemically and magnetically equivalent. To deal with the severe resonance signal overlap of H-2 with H-6_S, and H-4 with H-5, the experimental STD effect for both pairs was determined as a sum, *i.e.* H-2+H-6_S, and H-4+H-5. The calculated STD effects for those protons (H-2, H-6_S, H-4, H-5) was summed up pairwise in the same manner before calculating the NOE R -factor. The matching between the experimental STD effects and the calculated ones for pose 1 is excellent and consequently a remarkably low R -factor (0.07) was obtained for this model. The matching for the other two poses was worse as reflected by the higher R -factors (0.5 for pose 2 and 0.2 for pose 3). In view of these results it was concluded that pose 1 is the model which actually reflects the binding mode of **1** in the primary saccharide-binding site of WGA.

¹H and ⁷⁷Se NMR measurements with a solution of **1 in rabbit plasma**

Lyophilized rabbit plasma (containing 3.8% trisodium citrate as anticoagulant) was reconstituted in D₂O. The resulting hazy, yellowish solution was centrifuged to remove any insoluble debris. A 1.5 mM stock solution of glycosyldiselenide **1** in D₂O was prepared.

Reconstituted plasma and carbohydrate stock solutions were combined in a 1:2 ratio to yield a working solution with a 1 mM concentration of **1**. It is important to highlight that plasma samples for NMR metabolomic studies are typically diluted in the same way.²⁵

The solution of **1** in rabbit plasma was measured using two standard ¹H NMR pulse sequences for metabolomic profiling of serum/plasma samples, namely the 1D nuclear Overhauser effect spectroscopy with presaturation,²⁶ and the 1D Carr–Purcell–Meiboom–Gill (CPMG)²⁷ sequences. The first one is the prevalent option for solvent suppression reducing the residual water resonance signal while the second one is employed for suppression of macromolecular background signals on the basis of T_2 editing. First, a single pulse experiment with presaturation was carried out to determine the 90° pulse length and optimise the spectrometer frequency offset to minimise the residual solvent resonance, a recycle delay (RD) of 2 seconds and an acquisition time (AQ) of 3 seconds were employed. Then, the pulse sequence was changed to *noesygppld* (RD-90°-3 μ s-90°- t_m -90°-AQ) for more effective solvent suppression. A typical mixing time¹⁶ of 100 ms was employed with a total of 128 scans. The CPMG pulse sequence (RD-90°-(τ -180°- τ_n -AQ) with presaturation (*cpmgpld*) was employed for suppression of macromolecular signals on the basis of T_2 editing. Typical parameters for blood serum/plasma are τ =400 μ s and n =300 giving a total filter time of 240 ms which achieved the desired suppression of macromolecular signals

This sample was also measured by ⁷⁷Se NMR. The sensitivities of ¹³C and ⁷⁷Se are comparable in routine NMR experiments.²⁸ NMR spectra were acquired on a Bruker DRX500 spectrometer equipped with a 5-mm broadband BBO operating at a frequency of 95.406 MHz. Proton-decoupled (power-gated decoupling) ⁷⁷Se spectra were recorded using the *zgpg* pulse sequence from the spectrometer library with an spectral width of 57.5711 KHz, an acquisition time of 0.285 s, with 102,400 scans, relaxation delay of 2 s, a 90° pulse width of 12 μ s and standard waltz16 decoupling. Selenomethionine was used as an external secondary chemical shift reference standard, set at 68.1 ppm (dimethyl selenide as primary reference at 0 ppm).²⁸ Sample temperature was 298 K. Glycosyldiselenide **1** was cleanly observed at 407.9 ppm without any interference from the plasma matrix.

References

1. O. Boutureira, G. J. L. Bernardes, M. Fernández-González, D. C. Anthony and B. G. Davis, *Angew. Chem. Int. Ed.*, 2012, **51**, 1432.
2. O. Trott and A. J. Olson, *J. Comput. Chem.*, 2010, **31**, 455.

3. W. L. DeLano, *The PyMOL Molecular Graphics System*, (2002), DeLano Scientific: Palo Alto, CA.
4. (a) Y. Nishida, H. Ohrui and H. Meguro, *Tetrahedron Lett.*, 1984, **25**, 1575; (b) Y. Nishida, H. Hori, H. Ohrui and H. Meguro, *J. Carbohydr. Chem.*, 1988, **7**, 239; (c) K. Bock and J. Ø. Duus, *J. Carbohydr. Chem.*, 1994, **13**, 513.
5. A. Kristiansen, Å. Nysæter, H. Grasdalen and K. M. Vårum, *Carbohydr. Polym.*, 1999, **38**, 23.
6. D. LeVine, M. J. Kaplan and P. J. Greenaway, *Biochem. J.*, 1972, **129**, 847.
7. C. Wright and N. Raikhel, *J. Mol. Evol.*, 1989, **28**, 327.
8. M. Mayer and B. Meyer, *Angew. Chem. Int. Ed.*, 1999, **38**, 1784.
9. K. Lycknert, M. Edblad, A. Imberty and G. Widmalm, *Biochemistry*, 2004, **43**, 9647.
10. K. Fehér, R. P. Matthews, K. E. Kövér, K. J. Naidoo and L. Szilágyi, *Carbohydr. Res.*, 2011, **346**, 2612.
11. K. Stott, J. Stonehouse, J. Keeler, T.-L. Hwang and A. J. Shaka, *J. Am. Chem. Soc.*, 1995, **117**, 4199.
12. J. Angulo, C. Rademacher, T. Biet, A. J. Benie, A. Blume, H. Peters, M. Palcic, F. Parra and T. Peters, *Methods Enzymol.*, 2006, **416**, 12.
13. L. Fielding, *Prog. Nucl. Magn. Reson. Spectrosc.*, 2007, **51**, 219.
14. D. Schwefel, C. Maierhofer, J. G. Beck, S. Seeberger, K. Diederichs, H. M. Möller, W. Welte and V. Wittmann, *J. Am. Chem. Soc.*, 2010, **132**, 8704.
15. M. J. Potrzebowski, M. Michalska, J. Blaszczyk, M. W. Wieczorek, W. Ciesielski, S. Kazmierski and J. Pluskowski, *J. Org. Chem.*, 1995, **60**, 3139.
16. G. M. Morris, D. S. Goodsell, R. S. Halliday, R. Huey, W. E. Hart, R. K. Belew and A. J. Olson, *J. Comput. Chem.*, 1998, **19**, 1639.
17. D. Neumann, O. Kohlbacher, H.-P. Lenhof and C.-M. Lehr, *Eur. J. Biochem.*, 2002, **269**, 1518.
18. (a) V. Jayalakshmi and N. R. Krishna, *J. Magn. Reson.*, 2004, **168**, 36; (b) N. R. Krishna and V. Jayalakshmi, *Prog. Nucl. Magn. Reson. Spectrosc.*, 2006, **49**, 1.
19. S. Neal, A. Nip, H. Zhang and D. Wishart, *J. Biomol. NMR*, 2003, **26**, 215.
20. K. J. Neurohr, N. Lacelle, H. H. Mantsch and I. C. Smith, *Biophys. J.*, 1980, **32**, 931.
21. A. G. Palmer and D. A. Case, *J. Am. Chem. Soc.*, 1992, **114**, 9059.
22. M. Thépaut, C. Guzzi, I. Sutkeviciute, S. Sattin, R. Ribeiro-Viana, N. Varga, E. Chabrol, J. Rojo, A. Bernardi, J. Angulo, P. M. Nieto and F. Fieschi, *J. Am. Chem. Soc.*, 2013, **135**, 2518.
23. A. Bhunia, V. Jayalakshmi, A. J. Benie, O. Schuster, S. Kelm, N. Rama Krishna and T. Peters, *Carbohydr. Res.*, 2004, **339**, 259.
24. (a) S. Kemper, M. K. Patel, J. C. Errey, B. G. Davis, J. A. Jones and T. D. W. Claridge, *J. Magn. Reson.*, 2010, **203**, 1; (b) I. Pérez-Victoria, S. Kemper, M. K. Patel, J. M. Edwards, J. C. Errey, L. F. Primavesi, M. J. Paul, T. D. W. Claridge and B. G. Davis, *Chem. Commun.*, 2009, 5862.
25. O. Beckonert, H. C. Keun, T. M. D. Ebbels, J. Bundy, E. Holmes, J. C. Lindon and J. K. Nicholson, *Nat. Protocols*, 2007, **2**, 2692.
26. D. Neuhaus, I. M. Ismail and C.-W. Chung, *J. Magn. Reson. A.*, 1996, **118**, 256.
27. S. Meiboom and D. Gill, *Rev. Sci. Instrum.*, 1958, **29**, 688.
28. H. Duddack, *Prog. Nucl. Magn. Reson. Spectrosc.*, 1995, **27**, 1.